JOURNAL OF MECHANICAL ENGINEERING AND SCIENCES (JMES)
ISSN: 2289-4659 e-ISSN: 2231-8380
VOL. 14, ISSUE 4, 7348 – 7360
DOI: https://doi.org/10.15282/jmes.14.4.2020.03.0577

ORIGINAL ARTICLE

Effect of boundary factor and material property on single square honeycomb sandwich panel subjected to quasi-static compression loading

Quanjin Ma*[1,2], Tengfei Kuai[3], M.R.M.Rejab[1,2], Nallapaneni Manoj Kumar[4] and M.S.Idris[1]

[1] Structural Performance Materials Engineering Focus Group, Faculty of Mechanical & Automotive Engineering Technology, Universiti Malaysia Pahang, 26600 Pekan, Pahang, Malaysia
Phone: +60172667860; Fax: +6094246222
[2] School of Mechanical En gineering, Ningxia University, 750021 Yinchuan, China
[3] School of Mechanical Engineering, Nanjing University of Science and Technology, Nanjing 210094, China
[4] School of Energy and Environment, City University of Hong Kong, Kowloon, Hong Kong

ABSTRACT – This paper is aimed to investigate the crushing response of single square honeycomb panels under quasi-static compression loading. Two types of materials are used in this study, which refers to 100 % polylactic acid (PLA) and 70 % PLA filled 30 % carbon fibre (PLA/CF). Single honeycomb panels were fabricated through additive manufacturing technique, and assembled using slotting technique. The effect of boundary factor on the single square honeycomb panels have been studied, which refers to none, single-side, double-side boundary conditions. The effect of material properties on the crushing response has also involved. For the tensile test, it was concluded that the PLA/CF specimen offered the higher young modulus with 428.75 MPa than 360.76 MPa of PLA specimen. For the quasi-static compression test, the compressive modulus and strength of the single honeycomb sandwich panel showed 489.69 MPa and 18.32 MPa with boundary type 1, which provided the highest value compared to other two boundary condition types. Moreover, the square honeycomb sandwich panels with PLA/CF material and type 3 boundary condition offered the better crushing performance on energy absorption (*EA*) with 66.42 kJ and specific energy absorption (*SEA*) with 2282.47 kJ/kg. In addition, the crushing behaviour and failure mode were also involved and discussed in this study.

ARTICLE HISTORY
Received: 14th Sept 2019
Revised: 27th Apr 2020
Accepted: 14th May 2020

KEYWORDS
Compressive strength; crushing response; boundary factor; material property; honeycomb sandwich panel

INTRODUCTION

In recent years, composite material is increasingly used in numerous fields such as automotive, aerospace, military, and construction applications [1-5], which is due to its light-weight, low density, high strength-to-weight ratio, and better energy absorption properties [6, 7]. Sandwich panel generally consists of two high-stiffness thin sheets and a core structural panel with low-density materials. Several types of core structure have been investigated such as foams, periodic cellular, pyramidal truss and honeycomb structures used as structural applications [8-11]. Several geometric parameters of sandwich structure have been studied on sandwich structural panels such as core geometry, foam-filled, thickness and materials of skin sheet, and it obtains various mechanical properties and good energy-absorbing performance with high strength-to-weight ratio [12-15]. Among various core structures of sandwich panel, aluminium honeycomb structure offers great energy-absorbing performance under axial crushing conditions [16-18], which exhibits that sandwich honeycomb structure has a great application prospect.

Honeycomb structure is typically used as shock-absorbent purposes in automotive areas due to its anti-shock and higher energy-absorbing properties [19, 20]. Honeycomb structure is used as tailored solutions based on its design of neighbour core-connected structure [21, 22]. There are various studies on the mechanical properties of sandwich honeycomb panel. For example, Kobayash et al. studied the quasi-static and dynamic loading conditions on polyester (PET) and polypropylene (PP) thermoplastic honeycomb core, which found that dynamic test obtained a greater energy absorption compared to quasi-static test [23]. Yasui studied that the crushing behaviour of multi-layer honeycomb sandwich panels as pyramid-type panels, which showed the most effective design concept [24]. Alia et al. [25] investigated the compressive properties and energy-absorbing characteristics of carbon fibre reinforced honeycomb structure using the resin transfer method.

The new Nomex honeycomb core has been reinforced with small diameter composite rods to advance its mechanical properties, which has been studied by Alia et al. [26]. Like honeycomb structural materials, several researchers have developed the different types of materials to study its relevant mechanical properties. For instance, the low-velocity impact response of aluminium honeycomb sandwich structures has been investigated by conducting drop-weight impact tests by Md. Akil Hazizan [27]. Haydn N. G et al. [8] researched the new structure with periodic metallic sandwich panels by novel fabrication and topology design tools. Interestingly, S.A.H.Roslan et al. [28] conducted a triangular honeycomb core structure based on bamboo-epoxy composites using the slotting technique, which indicated that the triangular

*CORRESPONDING AUTHOR | Quanjin Ma | ✉ neromaquanjin@gmail.com

honeycomb bamboo / epoxy structure offered about 10 % more energy absorption than the square honeycomb structure. Z. Ansari reported the square honeycomb structure made out of sugar palm reinforced polylactic acid (PLA), which was 100 % bio-based material to improve its crushing response [29, 30]. The square and triangular honeycomb core materials based on co-mingled flax fibre reinforced PP and PLA polymers [31]. Therefore, it has a great potential to study on the lightweight and recycled materials on sandwich honeycomb such as polulactic acid, natural fibre reinforced composites [32], and hybrid polymers [33, 34].

Although some works have been carried out to investigate the crushing response of various sandwich panels with novel cores, there is limited works study on the compressive properties of single square honeycomb panels. Therefore, the aim of this paper has studied the effect of boundary factor and properties of single square honeycomb panels under quasi-static compression loading. Three types of boundary conditions have been studied on the crushing response of sandwich panel, which refers to none, single-side and double-side boundary types. Tensile tests are performed to obtain the tensile properties of two types of renewable materials. The compressive properties of the single square honeycomb sandwich panel are conducted under the quasi-static compression. Moreover, the crushing response of honeycomb panel with three boundary conditions are involved in this study.

METHODS AND MATERIALS

Material Preparation

Two types of filaments were provided, which were PLA and PLA/carbon fibre spools. PLA filament spool was supplied by Cixi Lanbo Printing Supplies Co., Ltd, China, which had a low shrinkage, thermoforming dimensional stability. The PLA/carbon fibre filament spool was obtained from Fabbxible Co., Ltd, which combined 70 % PLA and 30 % carbon fibre. Table 1 presents specifications of two types of filament spools used in this study. For 3D printing equipment [35], the Prusa i3 MK3 printing machine was used to manufacture tensile specimens, slot and skin plates. Moreover, AB epoxy type adhesive glue was used to bond the single square honeycomb core structure with skin plate.

Table 1. Several specifications of PLA and PLA/CF materials

Specifications	PLA	PLA/CF
Color	Yellow	Black
Density	1.24 g/cm^3	1.30 g/cm^3
Content ratio (%)	100 %	70 % PLA and 30 % carbon fibre
Diameter dimension (mm)	1.75 ± 0.05	1.75 ± 0.05
Extruder temperature	180-230 °C	210-230 °C
Bed temperature	20-60 °C	20-50 °C
Glass transition temperature	50 °C	50 °C

Note: PLA: Polylactic acid; PLA/CF: Polylactic acid mixed with carbon fibre

Fabrication Method

The Prusa i3 MK3 printing machine was used to manufacture all specimens in this study, which involved tensile specimens, the single slot, and square sandwich plates. Several setting parameters in PrusaSlicer software were set, which referred to the linear infill pattern and 50 % infill percentage. Tensile specimens with two types of materials were shown in Figure 1, which followed the ASTM 638-14 standard. Detailed design geometrical structure of the single slot and skin plates were illustrated in Figure 2. Three boundary condition types of honeycomb panels were fabricated, and the schematic diagram of three types was mainly shown in Figure 3. Three boundary type conditions have been defined and explained as follows. Type 1 is defined as the single honeycomb core structure unbonded without skin plates, which is also named free boundary conditions. Type 2 is regarded as the core structure bonded with skin plate at single side. Type 3 is recognized as the core structure bonded at double-sides with 2 skin plates. In this study, the thickness of skin plate was 3 mm, and it was exhibited the single-fixed and double-fixed boundary conditions on Type 2 and Type 3, respectively. The deformation of sandwich panels were attributed to the boundary condition, which was identified in this work.

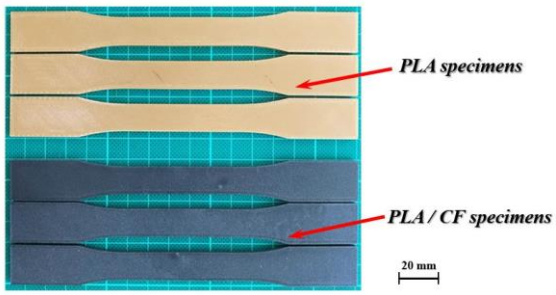

Figure 1. Specimens with PLA and PLA/CF materials for tensile test

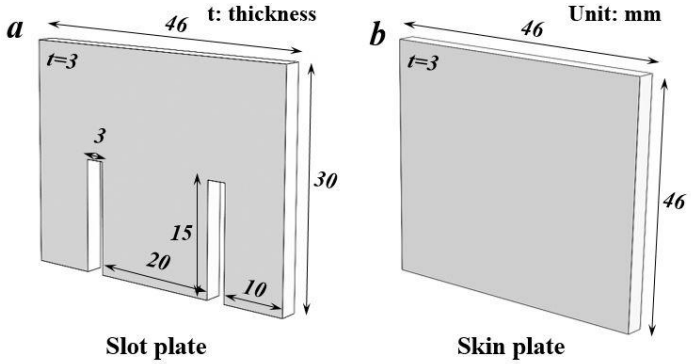

Figure 2. Detailed design of the single square sandwich panel: (a) slot plate and (b) skin plate

Fabrication procedure of the single honeycomb sandwich panels was also briefly exhibited in Figure 3, which was assembled following the direction of red arrows through the slotting technique. Skin plate was bonded with the single honeycomb core structure, and it was used AB epoxy type adhesive glue with epoxy resin (component A) and polyfunctional hardener (component B) mixing with the ratio of 1 : 1. Specimens were cured under the vertical loading of 5 kN for 12 hours curing stage, and overall specimens of honeycomb panels were summarized and shown in Figure 4, which referred to two types of materials and three boundary condition types. The construction of the sandwich panel was fabricated through the slots. Here, the mechanical responses were studied on the overall honeycomb structure, which was attributed to the interaction of the slots. The slots were compressed as the single honeycomb core without using any adhesive glues between two contact surfaces.

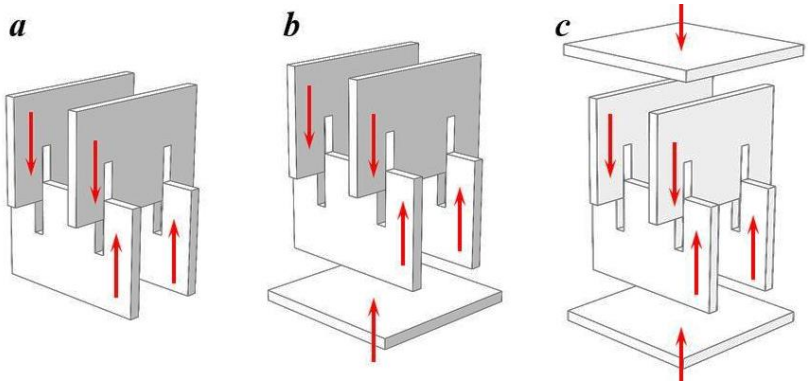

Figure 3. Three types of boundary conditions: (a) type 1, (b) type 2 and (c) type 3

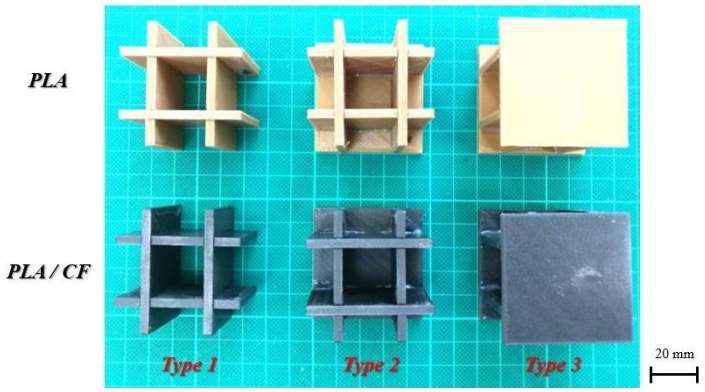

Figure 4. The single square honeycomb sandwich panels with three types of boundary conditions and two types of materials

Tensile Test

The tensile test was performed using the Instron 3369 model universal testing machine, which provided a maximum load capacity of 50 kN. Tensile specimens were followed by the ASTM D638 standard, which used 57 mm as the gage length [35]. At least three samples were carried out for each type. The tensile loading speed was set a 5 mm/min, and three specimens were prepared and carried out for two types of materials.

Quasi-static Compression Test

The quasi-static compression test was conducted using the Instron 3369 model universal testing machine, which followed the ASTM D1621 standard [36]. The single square honeycomb sandwich panels were placed between the two compression platens with a 2 mm/min crosshead speed. Three specimens of each material and boundary condition were used and conducted in this study, which considered the average value for further discussion. The specimens were crushed 70 % displacement of the initial core height, which were 21 mm, 23.1 mm and 25.2 mm for Type 1, 2 and 3, respectively. The crushing response was captured during the overall deformation stages, which recorded using the Nikon D3100 camera. At least three specimens were conducted for each condition. Figure 5 illustrates the schematic overview of honeycomb sandwich panels with three boundary condition types under the quasi-static compression loading. The brief summary of single square honeycomb sandwich panels is summarized in Table 2, which involves boundary type, material type, height, width and average mass. Here, ST1PLA of specimen ID represented sandwich panel with boundary condition type 1 used PLA material.

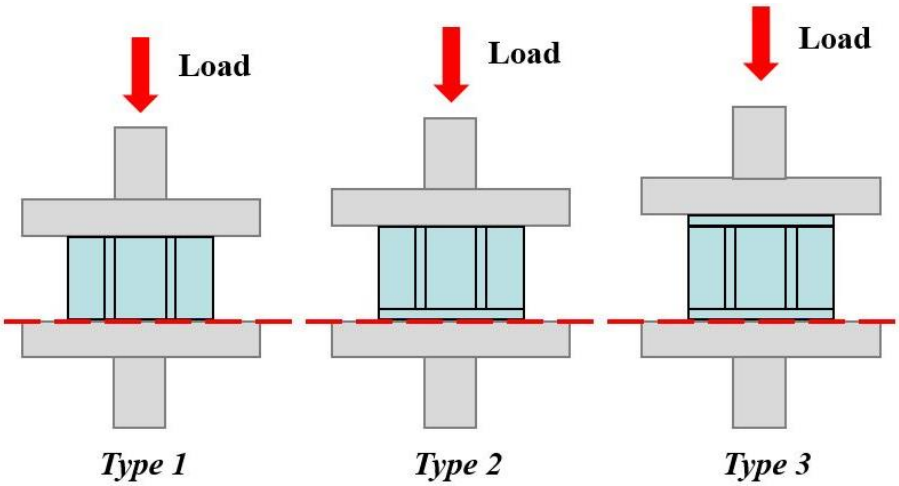

Figure 5. Schematic overview of the single honeycomb sandwich panel with three boundary condition types under quasi-static compression loading

Table 2. The summary of square honeycomb sandwich panels under quasi-static compression test

Specimen ID	Boundary condition type	Material type	Height (mm)	Width (mm)	Average mass (g)
ST1PLA	1	PLA	30	46	16.2
ST2PLA	2		33	46	22.3
ST3PLA	3		36	46	28.4
ST1PLACF	1	PLA/CF	30	46	15.9
ST2PLACF	2		33	46	22.4
ST3PLACF	3		36	46	29.1

RESULTS AND DISCUSSION

Result of Tensile Test

Graph of stress versus strain curves of PLA and PLA/CF materials were illustrated in Figure 6. PLA specimens exhibited an almost linear response under the elastic deformation stage. However, tested specimens were broken into two parts when started to undergo the initial plastic deformation stage. For PLA/CF materials, it showed a lower maximum tensile stress value and 1.18 times higher tensile modulus compared to PLA materials. Therefore, it is highlighted that PLA/CF specimens had a better plastic deformation response before it damaged. It was found that PLA/CF specimens could show 1.54 times higher nominal strain values compared to PLA specimens. It was shown that the PLA/CF material provided better stiffness comparing with PLA material.

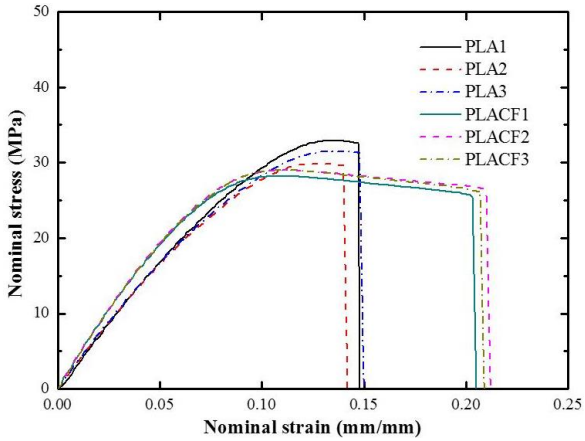

Figure 6. Typical stress versus strain curves of the PLA and PLA/CF specimens under tensile test

For two types of materials, the damaged fracture occurred approximately in the middle of the gauge length. However, the fracture characteristics of samples had the different fracture type and fracture location. For example, PLA specimens showed the shear fracture type, which attributed to material property. Typical damaged specimens of two materials were illustrated in Figure 7, which highlighted the damaged position and fracture type. Moreover, Table 3 summarizes the relevant results of tensile tests with two types of materials. The PLA/CF specimens had a higher young modulus of average value 428.75 MPa than the PLA specimens of average value 360.76 MPa, which provided the final nominal strain value with 0.21 and 0.14 used PLA and PLA/CF materials, respectively.

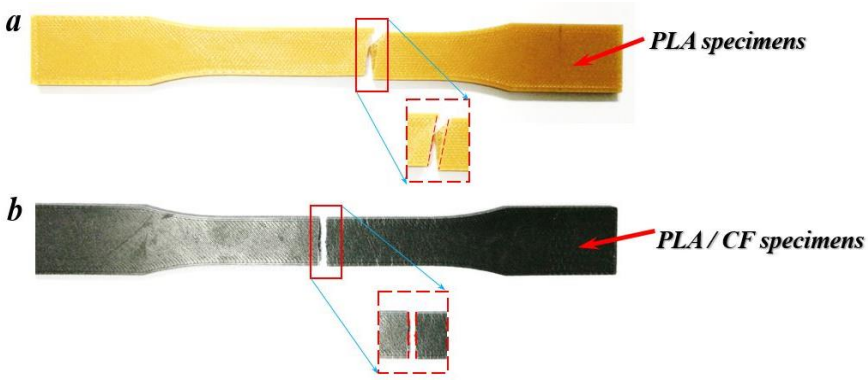

Figure 7. Damaged specimens under tensile test: (a) PLA specimen and (b) PLA/CF specimen

Table 3. Results of the tensile test with PLA and PLA/CF specimens

Specimen ID	Tensile modulus (MPa)	Elongation at break (%)	Maximum tensile stress (MPa)	Yield stress (MPa)
PLA1	369.02	0.13	32.92	17.23
PLA2	354.62	0.12	29.87	17.05
PLA3	358.63	0.13	31.51	17.12
PLACF1	429.02	0.20	28.23	12.21
PLACF2	430.91	0.21	28.98	12.02
PLACF3	426.32	0.20	29.05	12.07

Figure 8 presents the effect of the material property on young modulus and maximum stress under the tensile test, which is further used to compare and analyze the tensile properties with two types of materials. Therefore, the PLA/CF specimens offered a higher young modulus value and provided a lower maximum tensile stress compared to PLA specimens. Moreover, it is concluded that it is a sufficient method to advance the tensile properties of pure PLA material by adding the carbon fibre material [37].

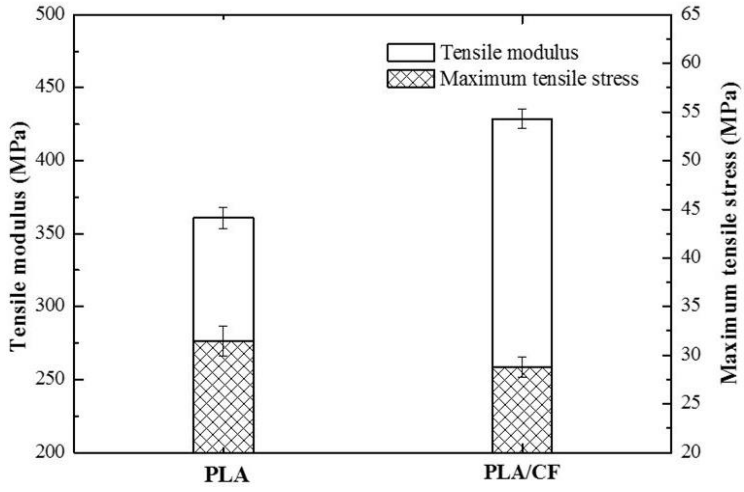

Figure 8. Effect of material property on tensile modulus and maximum stress

Result of Quasi-static Compression Test

The typical graph of load versus displacement curve of the single square honeycomb sandwich panel is shown in Figure 9. The crushing response of the single square honeycomb sandwich panel is divided into two deformation stages, which refer to the elastic and plastic stages. In the elastic deformation stage, the square honeycomb sandwich panel initially underwent the elastic deformation until the load shapely reached the maximum compression load. The square honeycomb sandwich panel presented the initial buckling at the slot plate closed to skin plate or in the middle of the slot

plate. In the plastic deformation stage, the applied loading rapidly decreased around 0.25 mm displacement, and the square honeycomb sandwich panel continued to buckle and deformed under continuous loading. With relative steady fluctuation of the minimum load, the applied load continued to increase with a slight trend until the sandwich panel was crushed the 70 % displacement of the initial height.

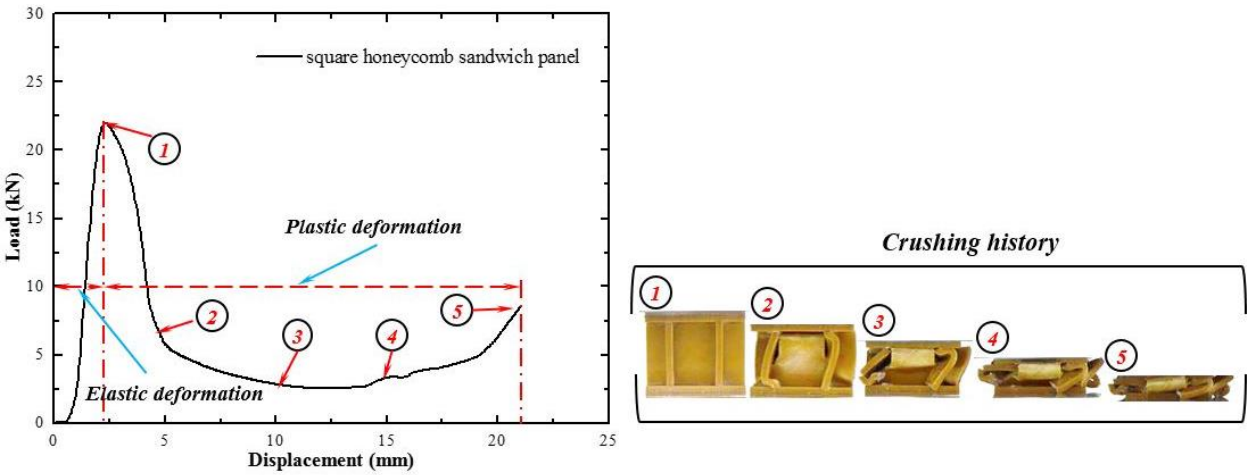

Figure 9. Graph of load versus displacement trace with crushing response under quasi-static compressive loading

The load versus displacement curves of the three boundary condition types were plotted in Figure 10. From the comparison result, it was concluded that the single square honeycomb panel with PLA material offered approximately 1.14 times peak load value than PLA/CF material at three boundary condition types. In addition, it presented a relative similar crushing response under the elastic and plastic deformation stages. Interestingly, it was highlighted that the single square honeycomb sandwich panel with PLA/CF material provided the better energy absorption and specific absorption energy under three different boundary condition types.

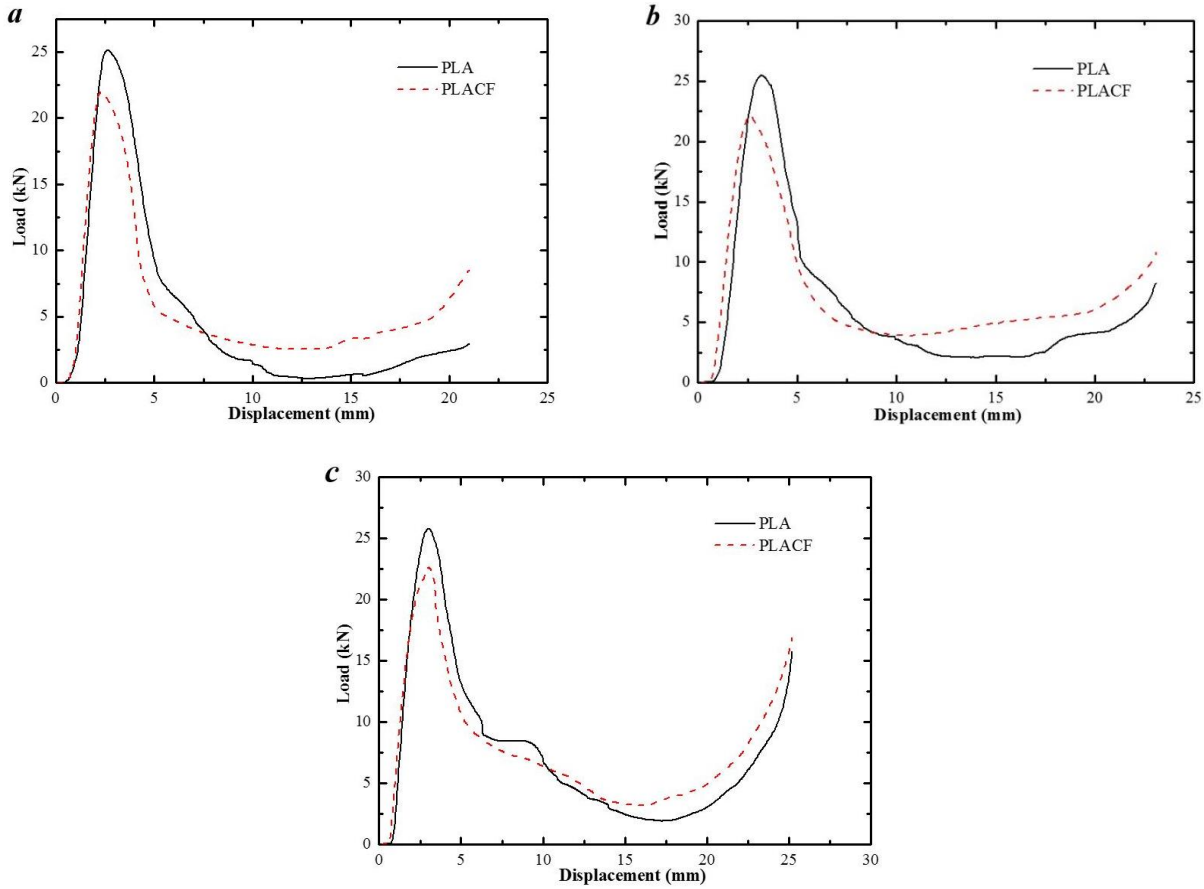

Figure 10. Load versus displacement traces of three boundary condition types with PLA and PLA/CF materials: (a) type 1, (b) type 2 and (c) type 3

Graphs of load versus displacement of the two materials under three different boundary condition types were plotted in Figure 11, which used to study the effect of boundary type used the same material. From Figure 11 (a) and (b), it was revealed that three boundary condition types offered a similar peak load under the same material type. Here, it was mentioned that the boundary factor of the single honeycomb sandwich panel had little effect under the elastic deformation stage.

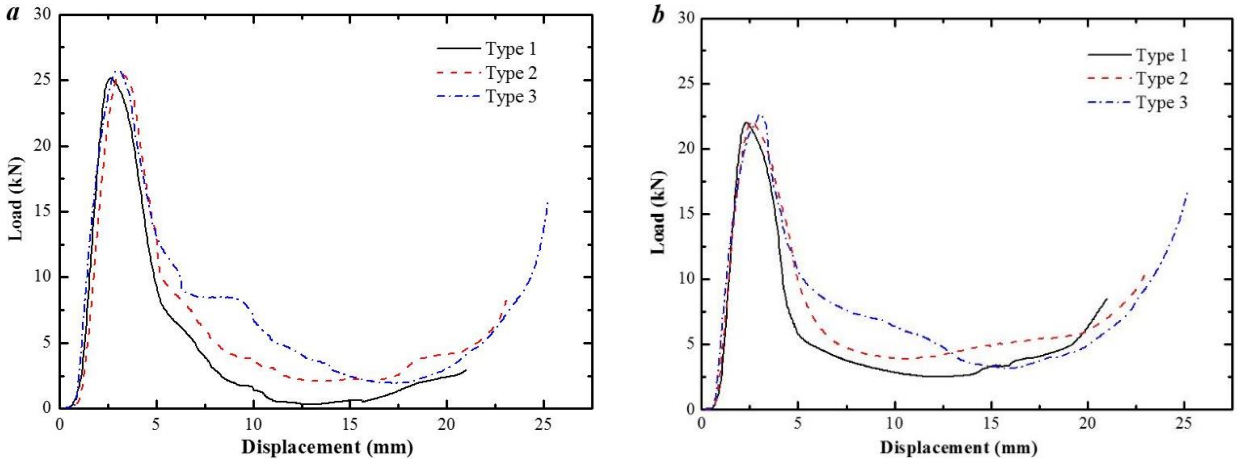

Figure 11. Graphs of load versus displacement with three boundary conditions: (a) PLA material and (b) PLA/CF material

With regard to its plastic deformation stage, it was mainly found that boundary type 3 offered better crushing performance compared to the other two types, which indicated the highest energy absorption and specific energy absorption values. The summary of compressive properties of the single square honeycomb sandwich panel with three boundary types were shown in Table 4, which involved compressive modulus and strength, yield strength, peak load (F_{peak}), energy absorption (*EA*) and specific energy absorption (*SEA*). The related parameters of the single square honeycomb sandwich panel were further discussed in detail.

Table 4. Summary of compressive properties of single square sandwich panel with three boundary conditions and two types of materials

Specimen ID	Compressive modulus (MPa)	Compressive strength (MPa)	Yield strength (MPa)	F_{peak} (kN)	*EA* (kJ)	*SEA* (kJ/kg)
ST1PLA	489.69	18.32	4.08	25.14	17.13	1057.40
ST2PLA	378.55	16.78	4.72	25.48	37.89	1699.12
ST3PLA	398.78	15.59	5.11	25.81	56.21	1979.22
ST1PLACF	461.56	15.93	2.88	21.98	30.47	1916.35
ST2PLACF	356.83	14.48	3.06	22.24	50.27	2244.19
ST3PLACF	364.23	13.10	4.36	22.69	66.42	2282.47

Figure 12 presented the effect of the boundary factor of the single square honeycomb sandwich panel on compressive modulus and strength with two types of materials. The compressive modulus and strength of the single honeycomb sandwich panel showed 489.69 MPa and 18.32 MPa on boundary type 1, which provided the highest value compared to the other two boundary condition types. Figure 12 (a) and (b) provided the same relationship trend with three boundary condition types. With three boundary condition types ranges from 1, 2 to 3 type, compressive strength exhibited the decreasing trend. Moreover, the compressive modulus value was minimum at the boundary type 2, which may due to the non-uniform boundary condition and friction between the structural cross-section wall and crosshead.

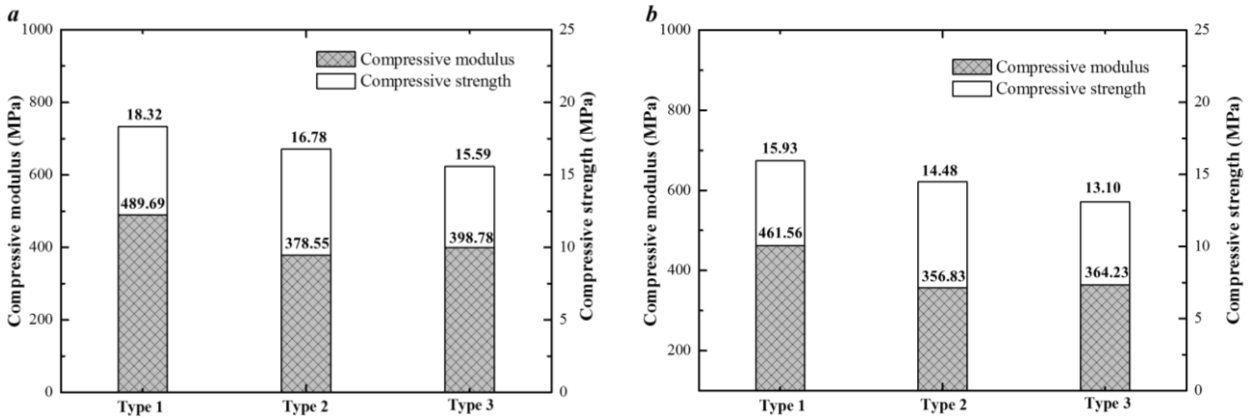

Figure 12. Effect of boundary factor on compressive strength and modulus: (a) PLA material and (b) PLA/CF material

Figure 13 (a) and (b) present the effect of the boundary type of the single square honeycomb sandwich panel on the peak load and yield strength. From Figure 13 (a) and (b), the highest average peak load was 25.81 MPa and 22.69 MPa for PLA and PLA/CF materials, which occurred at the boundary condition type 3. For yield strength, boundary condition type 3 showed the highest yield strength, which was 5.11 MPa and 4.36 MPa for PLA and PLA/CF materials. It was found that the boundary factor had a small effect on the peak load and yield strength of the single honeycomb sandwich panel. With the boundary condition type ranges from type 1, 2 and 3, it showed the slight increasing trend, and the maximum yield strength and yield strength at boundary condition type 3 of the single honeycomb sandwich panel.

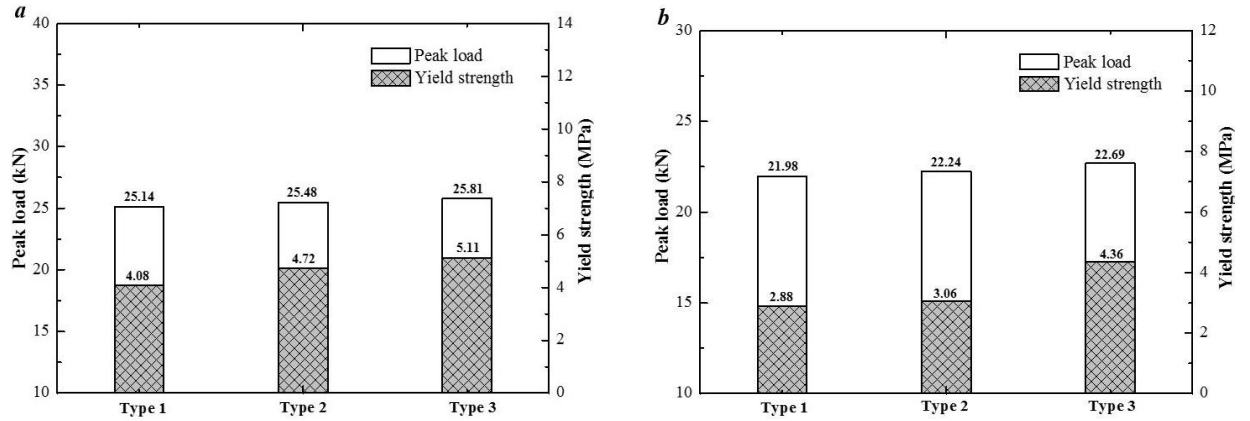

Figure 13. Effect of boundary condition type on peak load and yield strength: (a) PLA material and (b) PLA/CF material

The crushing response of the single square honeycomb sandwich panel was carried out, which referred to energy absorption and specific energy absorption. The specific energy absorption was calculated from the area under the load versus displacement over the mass of the specimen. Figure 14 illustrated the effect of boundary condition type of honeycomb sandwich panel on *EA* and *SEA*. With the boundary condition type number increased, *EA* and *SEA* exhibited slightly increasing trend as shown in Figure 14 (a) and (b), which refers to PLA and PLA/CF materials, respectively. The *EA* and *SEA* values were obtained the maximum values at boundary condition type 3. It was obtained that PLA/CF material offered a better crushing response on *EA* and *SEA*, which showed 1.18 times and 1.15 times value on *EA* and *SEA* compared to the single honeycomb sandwich panel with PLA material.

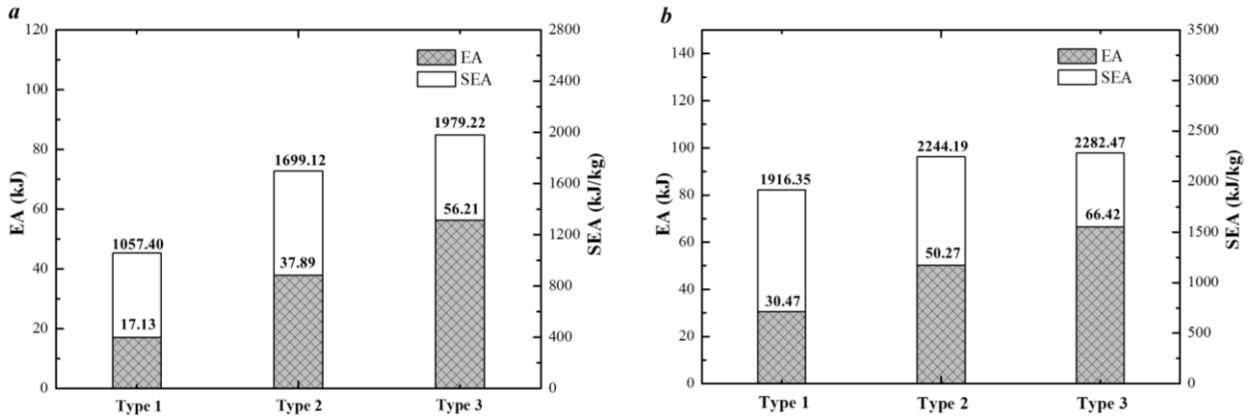

Figure 14. Effect of boundary type on energy absorption and specific energy absorption: (a) PLA material and (b) PLA/CF material

The crushing response of the single square honeycomb sandwich panel with three boundary conditions and two types of materials were shown in Figure 15. Three boundary condition types have three different interactive effects of the single honeycomb sandwich panel under quasi-static compression loading. It was found that the crushing deformation was briefly divided into two types, which were buckling and shear deformation modes. For boundary condition type 1 and 2, buckling mode mainly occurred. For boundary condition type 3, buckling mode occurred, and the core structure showed the shear deformation mode due to the interactive effect of two skin plates. Few small corner parts of the single slot plate were buckled and separated from the main core structure. For boundary condition type 2 and 3, a series of folds were observed in the middle part of the single slot plate between the two skin plates. Several debonding modes occurred at the bonding point between the core structure and skin plate.

Moreover, boundary condition type 2 and 3 of the single square honeycomb sandwich panels were stable in comparison with the boundary type 1, which referred to Figure 15 and 16. In addition, it was noted that all specimens exhibited the progressive deformation and gradually crushed into several folds. In this study, the crushing mechanisms were mainly attributable to buckling, folds, delamination, shear deformation, debonding, and failure cracks, which agreed with similar studies on honeycomb sandwich panels from the previous literatures [28-30].

The damaged specimens with three boundary types of square honeycomb sandwich panels were shown in Figure 16. Evidently, the boundary condition type of the square honeycomb sandwich panel largely affected the failure behaviour and plastic deformation mode, which appeared to be more significant than the effect of the material property. It was observed that the buckling and folds spread outward due to the restriction from the internal slot intervals. Subsequently, failure cracks were caused by the local stress concentration on the square honeycomb sandwich panel. In this study, the damaged single square honeycomb sandwich panels provided the similar failure deformation compared to the previous studies [28-30].

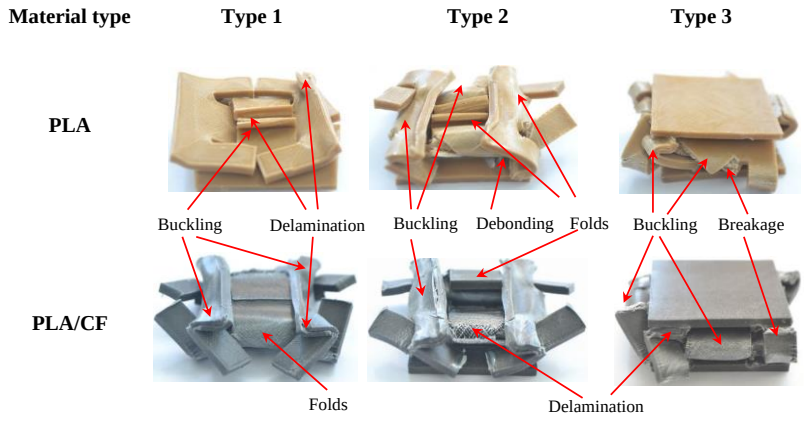

Figure 16. Damaged the single square honeycomb sandwich panels with three boundary types and two types of materials

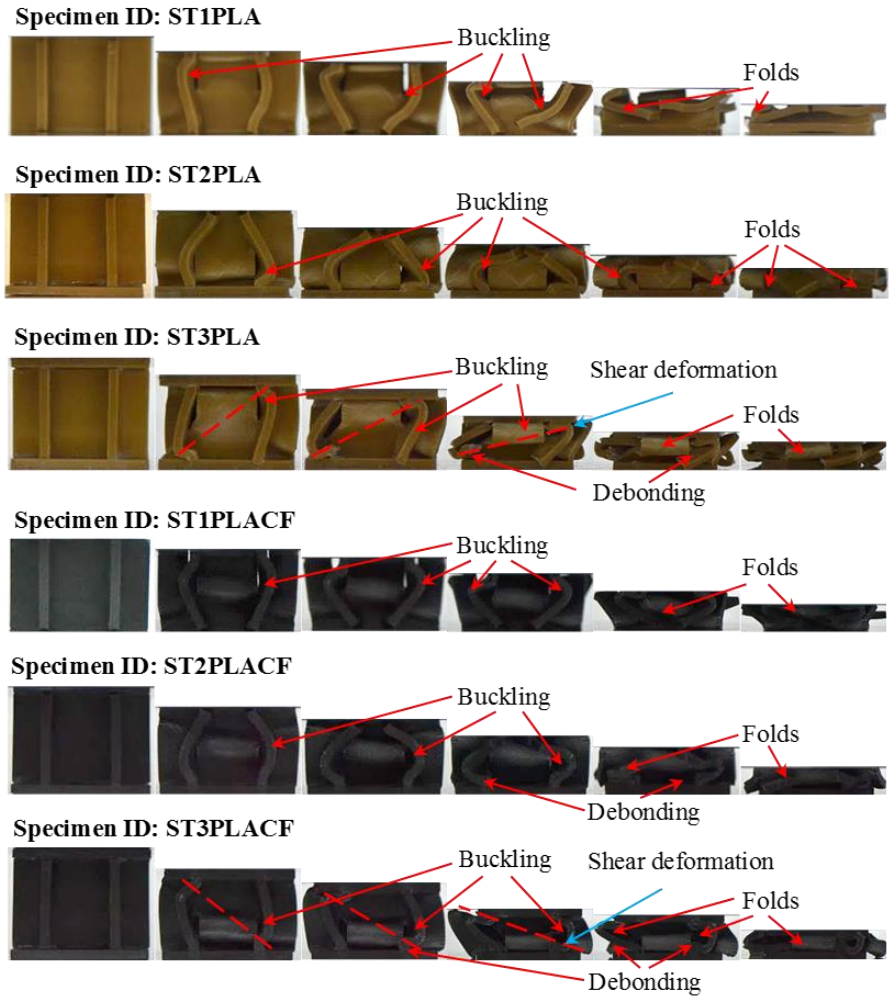

Figure 15. Photographs of crushing response of the single square honeycomb sandwich panels with three boundary types and two types of materials

CONCLUSIONS

The mechanical properties of the single square honeycomb sandwich panels with PLA and PLA/CF materials were carried out, which conducted under tensile test and quasi-static compressive test. The crushing response, load versus displacement curves, the effect of material and boundary factor were explored in this study. The conclusions are summarized as follows:

1) For the tensile test, it is concluded that the PLA/CF material provides 1.18 times tensile modulus compared to PLA material. In addition, it is showed that PLA/CF material offers 1.54 times higher nominal strain values compared to PLA material.

2) For the quasi-static compression test, it is obtained that the single square honeycomb with PLA material provides around 1.14 times higher value on peak load value than PLA/CF material with three boundary condition types. Furthermore, it is found that PLA/CF material of the single square honeycomb sandwich panel could offer a better crushing response on *EA* and *SEA*, which is 1.18 times and 1.15 times compared to PLA material.

3) The crushing response of the single square honeycomb sandwich panels is mainly observed the buckling, folds, delamination, breakage, and debonding in the plastic deformation stage.

ACKNOWLEDGMENTS

The authors would like to acknowledge the Ministry of Education Malaysia: FRGS/1/2019/TK03/UMP/02/10 and Faculty of Mechanical & Automotive Engineering Technology, Universiti Malaysia Pahang (UMP) for funding this research: PGRS180319. The first author (Quanjin Ma) is thankful to receive the *DRS (Doctorial Research Scheme) Scholarship* from *Institute of Postgraduate Studies*, *Universiti Malaysia Pahang*, *Malaysia*. This research work is strongly

supported by the *Structural Performance Materials Engineering (SUPREME) Focus Group* and the *Human Engineering Focus Group (HEG)* on research materials and equipment.

REFERENCES

[1] N. Z. M. Zaid, M. R. M. Rejab, and N. A. N. Mohamed, "Sandwich structure based on corrugated–core: A review," in *MATEC Web of Conferences: EDP Sciences*, 2016.

[2] M. Sun, D. Wowk, C. Mechefske, IY. Kim, "An analytical study of the plasticity of sandwich honeycomb panels subjected to low–velocity impact," *Composites Part B*, vol. 168, no. 1, pp. 121–128, 2019, doi: 10.1016/j.compositesb.2018.12.071.

[3] M. Sun, P. Kendall, D. Wowk, IY. Kim, C. Mechefske, "Damage assessment on the surface and honeycomb core of the aluminum sandwich panel subjected to low–velocity impact," in *ASME 2018 International Design Engineering Technical Conferences and Computers and Information in Engineering Conference: American Society of Mechanical Engineers*, 2018, pp. 1–7.

[4] M. Quanjin, M. R. M. Rejab, I. Sahat, M. Amiruddin, D. Bachtiar, J. P. Siregar, and M. I. Ibrahim, "Design of portable 3–axis filament winding machine with inexpensive control system," *Journal of Mechanical Engineering and Sciences*, vol. 12, no. 1, pp. 3479–3493, 2018, doi: 10.15282/jmes.12.1.2018.15.0309.

[5] M. Quanjin, M. R. M. Rejab. M. S. Idris, S. A. Hassan, and N. M. Kumar, "Effect of winding angle on the quasi–static crushing behaviour of thin–walled carbon fibre–reinforced polymer tubes," *Polymers and Polymer Composites.*, 2019, doi: 10.1177/0967391119887571.

[6] C. J. Shen, G. Lu, T. X. Yu, "Dynamic behavior of graded honeycombs–A finite element study," *Composite Structures.*, vol. 98, pp. 282–293, 2013, doi: 10.1016/j.compstruct.2012.11.002.

[7] D. Asprone, F. Auricchio, C. Menna, S. Morganti, A. Prota, A. Reali, "Statistical finite element analysis of the buckling behavior of honeycomb structures," *Composite Structures.*, vol. 105, pp. 240–255, 2013, doi: 10.1016/j.compstruct.2013.05.014.

[8] H. N. G. Wadley, N. A. Fleck, A. G. Evans, "Fabrication and structural performance of periodic cellular metal sandwich structures," *Composites Science and Technology*, vol. 63, no. 16, pp. 2331–2343, 2003, doi: 10.1016/S0266-3538(03)00266-5.

[9] B. L. Buitrago, C. Santiuste, S. Sánchez-Sáez, E. Barbero, C. Navarro, "Modelling of composite sandwich structures with honeycomb core subjected to high–velocity impact," *Composite Structures*, vol. 92, no. 9, pp. 2090–2096, 2010, doi: 10.1016/j.compstruct.2009.10.013.

[10] K. P. Dharmasena, H. N. G. Wadley, Z. Xue, J. W. Hutchinson, "Mechanical response of metallic honeycomb sandwich panel structures to high–intensity dynamic loading," *International Journal of Impact Engineering*., vol. 35, no. 9, pp. 1063–1074, 2008, doi: 10.1016/j.ijimpeng.2007.06.008.

[11] J. Xiong, L. Ma, S. Pan, L. Wu, J. Papadopoulos, A. Vaziri, "Shear and bending performance of carbon fiber composite sandwich panels with pyramidal truss cores," *Acta Materialia.*, vol. 60, no. 4, pp. 1455–1466, 2012, doi: 10.1016/j.actamat.2011.11.028.

[12] A. Petras, M. P. F. Sutcliffe, "Failure mode maps for honeycomb sandwich panels," *Composite Structures*, vol. 44, no. 4, pp. 237–252, 1999, doi: 10.1016/S0263-8223(98)00123-8.

[13] V. N. Burlayenko, T. Sadowski, "Effective elastic properties of foam–filled honeycomb cores of sandwich panels," *Composite Structures*, vol. 92, no. 12, pp. 2890–2900, 2010, doi: 10.1016/j.compstruct.2010.04.015.

[14] M. He, W. Hu, "A study on composite honeycomb sandwich panel structure," *Materials & Design.*, vol. 29, no. 3, pp. 709–713, 2008, doi: 10.1016/j.matdes.2007.03.003.

[15] M. R. M. Rejab. D. Bachtiar, J. P. Siregar, P. Paruka, S. Fadzullah, B. Zhang, "The mechanical behavior of foam–filled corrugated core sandwich panels in lateral compression," in *Proceedings of the American Society for Composites: Thirty-First Technical Conference*, 2016.

[16] M. K. Khan, T. Baig, S. Mirza, "Experimental investigation of in–plane and out–of–plane crushing of aluminum honeycomb," *Materials Science and Engineering A.*, vol. 539, no. 30, pp. 135–142, 2012, doi: 10.1016/j.msea.2012.01.070.

[17] I. Ivañez, L. M. Fernandez–Cañadas, S. Sanchez–Saez, "Compressive deformation and energy–absorption capability of aluminium honeycomb core," *Composite Structures*, vol. 174, no. 15, pp. 123–133, 2017, doi: 10.1016/j.compstruct.2017.04.056.

[18] A. P. Meran, T. Toprak, A. Muğan, "Numerical and experimental study of crashworthiness parameters of honeycomb structures," *Thin-Walled Struct.*, vol. 78, pp. 87–94, 2014, doi: 10.1016/j.tws.2013.12.012.

[19] W. A. D. W. Dalina, M. Mariatti, Z. A. M. Ishak, A. Mohamed, "Comparison of properties of mwcnt/carbon fibre/epoxy laminated composites prepared by solvent spraying method," *International Journal of Automotive and Mechanical Engineering*, vol. 10, pp. 1901–1909, 2014, doi: 10.15282/ijame.10.2014.7.0158.

[20] H. R. Sankar, R. R. Srikant, P. V. Krishna, V. B. Rao, P. B. Babu, "Estimation of the dynamic properties of epoxy glass fabric composites with natural rubber particle inclusions," *International Journal of Automotive and Mechanical Engineering*, vol. 7, pp. 968–980, 2013, doi: 10.15282/ijame.7.2012.13.0078.

[21] Z. S. Nazirah, M. S. Abdul Majid, R. Daud, "Effects of elevated temperatures on glass reinforced epoxy pipes under multi–axial loadings," *Journal of Mechanical Engineering and Sciences*, vol. 10, no. 1, pp. 1846–1856, 2016, doi: 10.15282/jmes.10.1.2016.9.0177.

[22] N. Fatchurrohman, S. Sulaiman, S. M. Sapuan, M. K. A. Ariffin, B. T. H. T. Baharuddin, "Analysis of a metal matrix composites automotive component," *International Journal of Automotive and Mechanical Engineering*., vol. 11, pp. 2531–2540, 2015, doi: 10.15282/ijame.11.2015.32.0213.

[23] H. Kobayashi, M. Daimaruya, T. Kobayashi, "Dynamic and static compression tests for paper honeycomb cores and absorbed energy," *JSME Journal of Solid Mechanics and Materials Engineering*, vol. 41, no. 3, pp. 338–344, 1998, doi: 10.1299/jsmea.41.338.

[24] Y. Yasui, "Dynamic axial crushing of multi–layer honeycomb panels and impact tensile behavior of the component members," *International Journal of Impact Engineering*., vol. 24, no. 6–7, pp. 659–671, 2000, doi: 10.1016/S0734-743X(99)00174-8.

[25] R. A. Alia, O. Al-Ali, S. Kumar, W. J. Cantwell, "The energy–absorbing characteristics of carbon fiber–reinforced epoxy honeycomb structures," *Journal of Composite Materials*, vol. 53, no. 9, pp. 1145–1157, 2019, doi: 10.1177/0021998318796161.

[26] R. A. Alia, S. Rao, R. Umer, J. Zhou, C. Zheng, Z. Guan, and W. J. Cantwell, "The crushing characteristics of reinforced Nomex honeycomb," *Journal of Reinforced Plastics and Composites.*, vol. 37, no. 20, pp. 1267–1276, 2018, doi: 10.1177/0731684418793211.

[27] M. A. Hazizan, W. J. Cantwell, "The low–velocity impact response of an aluminium honeycomb sandwich structure," *Composites Part B: Engineering*, vol. 34, no. 8, pp. 679–687, 2003, doi: 10.1016/S1359-8368(03)00089-1.

[28] S. A. H. Roslan, M. Z. Hassan, Z. A. Rasid, S. A. Zaki, Y. Daud, S. Aziz, and Z. Ismail, "Mechanical properties of bamboo reinforced epoxy sandwich structure composites," *International Journal of Automotive and Mechanical Engineering*, vol. 12, pp. 2882–2892, 2015, doi: 10.15282/ijame.12.2015.7.0242.

[29] Z. Ansari, M. R. M. Rejab, D. Bachtiar, J. P. Siregar, "Crushing response of green square honeycomb structure from sugar palm & PLA," in *Materials Science Forum: Trans. Tech. Publ.*, 2017, pp. 122–126.

[30] Z. Ansari, C. W. Tan, M. R. M. Rejab, D. Bachtiar, J. P. Siregar, M. Y. M. Zuhri, and N. Marzuki, "Crushing behaviour of composite square honeycomb structure: A finite element analysis," *Journal of Mechanical Engineering and Sciences*, vol. 2, pp. 2637–2649, 2017, doi: 10.15282/jmes.11.2.2017.7.0241.

[31] M. Y. M. Zuhri, Z. W. Guan, W. J. Cantwell, "The mechanical properties of natural fibre based honeycomb core materials," *Composites Part B: Engineering*, vol. 58, pp. 1–9, 2014, doi: 10.1016/j.compositesb.2013.10.016.

[32] A. F. Jusoh, M. R. M. Rejab, J. P. Siregar, D. Bachtiar, "Natural fiber reinforced composites: A review on potential for corrugated core of sandwich structures," in *MATEC Web of Conferences: EDP Sciences*, 2016.

[33] M. Quanjin, I. M. Sahat, M. R. M. Rejab, M. R, S. A. Hassan, B. Zhang, M. N. M. Merzuki, "The energy–absorbing characteristics of filament wound hybrid carbon fiber–reinforced plastic/polylactic acid tubes with different infill pattern structures," *Journal of Reinforced Plastics and Composites*, vol. 38, no. 23–24, pp. 1067–1088, 2019, doi: 10.1177/0731684419868018.

[34] M. Quanjin, M. S. A. Salim, M. R. M. Rejab, O. E. Bernhardi, A. Y. Nasution, "Quasi–static crushing response of square hybrid carbon/aramid tube for automotive crash box application," *Materials Today: Proceedings.*, 2019, doi: 10.1016/j.matpr.2019.10.161.

[35] M. Quanjin, M. R. M. Rejab, M. S. Idris, N. M. Kumar, M. Abdullah, G. R. Reddy, "Recent 3D and 4D intelligent printing technologies: A comparative review and future perspective," *Procedia Computer Science*, vol. 167, pp. 1210–1219, 2020, doi: 10.1016/j.procs.2020.03.434.

[36] M. Quanjin, M. R. M. Rejab, Q. Halim, M. N. M. Merzuki, M. Darus, "Experimental investigation of the tensile test using digital image correlation (DIC) method," *Materials Today: Proceedings.*, 2020, doi: 10.1016/j.matpr.2019.12.072.

[37] Standard. A. D1621, "Standard test method for compressive properties of rigid cellular plastics," West Conshohocken, *PA: ASTM International*, 2004.

[38] R. T. L. Ferreira, I. C. Amatte, T. A. Dutra, D. Bürger, "Experimental characterization and micrography of 3D printed PLA and PLA reinforced with short carbon fibers," *Composites Part B: Engineering.*, vol. 124, no. 1, pp. 88–100, 2017, doi: 10.1016/j.compositesb.2017.05.013.